Chapter 12
Plasmonic Hybrid Nanocomposites for Plasmon-Enhanced Fluorescence and Their Biomedical Applications

Ahmed Nabile Emam, Ahmed Sadek Mansour, Mona Bakr Mohamed, and Gehad Genidy Mohamed

Contents

Abstract Fluorescence is a powerful tool in biochemistry, biophysics, forensic science, and biotechnology. Two main principal properties for any fluorophore, brightness and photostability, are fundamentally important to achieve a high level of sensitivity for detection. Therefore, improvements in the technique are strongly

A. N. Emam (✉)
Refractories, Ceramics and Building Materials Department, National Research Centre (NRC), Cairo, Dokki, Egypt

Egyptian Nanotechnology Centre (EGNC), Cairo University, El-Sheikh Zayed City, 6th of October, Giza, Egypt

A. S. Mansour · M. B. Mohamed
National Institute of Laser Enhanced Sciences (NILES), Cairo University, Giza, Egypt

Egyptian Nanotechnology Centre (EGNC), Cairo University, El-Sheikh Zayed City, 6th of October, Giza, Egypt

G. G. Mohamed
Egyptian Nanotechnology Centre (EGNC), Cairo University, El-Sheikh Zayed City, 6th of October, Giza, Egypt

Chemistry Department, Faculty of Science, Cairo University, Giza, Egypt

H. K. Daima et al. (eds.), *Nanoscience in Medicine Vol. 1*, Environmental Chemistry for a Sustainable World 39,
https://doi.org/10.1007/978-3-030-29207-2_12

encouraged and pursued, such as new developments in terms of the technique sensitivity, the range of fluorophores, their stability, and the versatility of the experimental setups that help move this particular scientific research in biosensing and molecular imaging forward. Therefore, a new avenue is based on the use of plasmonic nanostructures in the enhancement of the collective photo-physical properties including their absorption and fluorescence, known as "plasmon-enhanced fluorescence." Such plasmonic enhancement is due to the localized surface plasmon resonance at the metal surface, which leads to increasing the exciton radiative recombination rate in the fluorophore and thereby improves the signal obtained and increases sensitivity. In addition, the plasmonic enhancement might depend on several parameters such as nanoparticle size and shape, metal type, and the spectral overlap in the absorption spectra and the type and the separation distance between both plasmonic nanoparticle and the fluorophore. Throughout this chapter, previous approaches are discussed, which are devoted to tracking the influence of plasmonic nanostructures on the photoluminescence of the fluorophores especially the hybrid nanocomposites based on plasmonic/quantum dots including semiconductor and carbon-based nanoparticles. In addition, the possible applications of metal-enhanced fluorescence nanohybrids in the biological and medical applications such as imaging and biosensing techniques.

Keywords Metal-enhanced fluorescence · Plasmonic nanostructures · Fluorophores · Carbon dots · Quantum dots · Hybrid nanocomposites · Biosensing · Biomedical imaging

12.1 Introduction

Fluorescence spectroscopy is a widely employed technique for chemical analysis, biochemistry, biophysics, forensic science, biosensing, and biotechnology because of its inherent high sensitivity, and its large linear concentration ranges, often significantly larger than in absorption methods, but the latter find more applicability as relatively few species exhibit fluorescence (Skoog et al. 2017; Lakowicz 2013). Recently fluorescence has become a primary methodology in life sciences because of its sensitivity, ease of use, and versatility (Xie et al. 2008). It has been used as an imaging tool in the clinical diagnosis and monitoring processes in biological systems (Bardhan et al. 2009).

Particularly, molecular fluorescence is a luminescence process that occurs when an atom or molecule relaxes to its ground state, after being excited, by emitting light. A molecule that is capable of fluorescence is called a fluorophore. When light from an external source interacts with the fluorophore, the fluorophore absorbs the light energy, resulting in a higher energy state. As the excited fluorophore is unstable at higher energy states, it relaxes from its higher energy state to a meta-stable state via small non-radiative transitions and then finally releases its excess energy from the meta-stable excited state to the ground state via a radiative transition through the process of emission of light. The light energy emitted by a fluorophore

is always longer in wavelength than the light energy absorbed, due to some non-radiative energy loss during its transition to the ground state. Therefore, a lot of studies have been performed to achieve high fluorescence yields (Xie et al. 2008).

The understanding of the interaction of light with matter allows us to design and apply the mechanism into applications. Thus, it is necessary to properly understand how the light interacts with the matter and then design structures that allow optimum conversion of light into the specific application (Piccione et al. 2014). A wide range of methods has been developed for enhanced fluorescence to increase the sensitivity of fluorescence, such as optical fiber fluorescence detectors. Of all the methodologies, metal-enhanced fluorescence (MEF) has been the most widely investigated and explored. The attractive changes in fluorescent properties of fluorophores due to this MEF include increased rates of excitation, increased quantum yields, and decreased fluorescence lifetimes with an increased photostability. The presence of these metallic structures in the vicinity of the fluorophore can alter the optical properties of the fluorophore by increasing the excitation field depending on the distance between the metal nanoparticle and fluorophore (Geddes 2013).

Advancement in nanotechnology allows us to create nanoscale structures (Aslan et al. 2005; Rosi and Mirkin 2005; Katz and Willner 2004). As the size of the metal is reduced too much smaller than the wavelength of the incoming light, a localized collective oscillation of electrons occurs in metals (Lakowicz et al. 2004; Stoermer and Keating 2006). This is now commonly known as localized surface plasmon resonance (LSPR). This phenomenon has opened diverse opportunities in technology advancement, ranging from arts, science, medical, and engineering (Geddes et al. 2005; Touahir et al. 2010).

This chapter is devoted to exploring the photo-physical properties of plasmonic nanostructure based on the LSPR, in addition to the factors that determine the strength of LSPR such as the density of electrons, the effective electron mass, the shape, and size of the charge distribution. Furthermore, the influence of the LSPR on the fluorescence properties of the fluorophores such as organic dyes, quantum dots, and carbon dots has been demonstrated. In addition, the required criteria to achieve the metal-enhanced fluorescence phenomena has been discussed. Finally, an overview of the achieved work was done by our research group and others regarding using of engineered hybrid nanocomposites to achieve a MEF mechanism and their possible applications in the biomedical field such as biosensing and bioimaging.

12.2 Plasmonic Nanoparticles

12.2.1 Surface Plasmon

Surface plasmons originate from free collective charge oscillations on metallic surfaces. There are two types of plasmon modes on metallic surfaces, namely localized surface plasmons (LSPR) (Haes and Van Duyne 2002; Hutter and Fendler 2004; Willets and Van Duyne 2007) and propagating surface plasmons also referred to as

surface plasmon polaritons (SPP). LSPR are observed at an optical wavelength for subwavelength-sized particles, while surface plasmon polaritons are observed on flat or corrugated continuous surfaces (Pitarke et al. 2006).

Localized Surface Plasmon Resonance

LSPR is a subfield of plasmonics that is associated with resonances due to noble metal nanostructures which cause spectral absorption, scattering peaks, and strong electromagnetic (EM-field) near-field enhancements (Haes and Van Duyne 2002). Localized surface plasmon can be excited directly by an incident light beam. The oscillating electromagnetic field associated with the incident light interacts with the conduction electrons in the metal particle and displaces them with respect to the ionic lattice of the metal (**see** Fig. 12.1) (Mayer and Hafner 2011). Upon displacement of the electrons, an attracting force arises that pulls the electrons back into equilibrium. Thus the metal nanoparticle can be seen as an oscillating system, where the light represents an external force, which drives an oscillator. As a typical oscillating system, metallic nanoparticles exhibit resonance frequencies (Hutter and Fendler 2004; Willets and Van Duyne 2007). The resonance frequency (or resonance wavelength) is dependent on the size, the shape, the metal used, and the dielectric environment surrounding the metal nanoparticle. Highest fields at the surface of nanoparticles can be observed when the incident light has the same wavelength as the resonance wavelength (Haes and Van Duyne 2002).

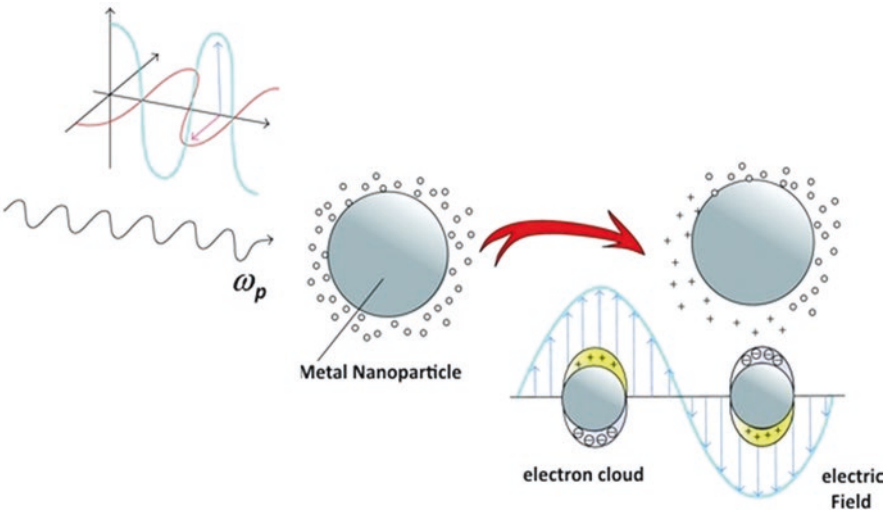

Fig. 12.1 Localized surface plasmon resonance (LSPR) of noble metal (Ag, Au) nanoparticles, a collective electron density oscillation caused by the electric field component of incoming light. (Reprinted with a Copyright permission from Anna Zielińska-Jurek 2014)

The interaction between those metal nanoparticles and the incoming light results can result in absorption of energy by the nanoparticles (generation of heat) or elastic scattering of light back to space (Mie 1908). Mie theory describes the EM-field enhancement within and out of the spherical particle and allows calculation of the scattering cross section $\sigma_{sca,}$ absorption cross section σ_{abs}, and extinction cross section σ_{ext}. The scattering cross section describes the ability to scatter the incident light into different directions with respect to the incident plane wave, while the absorption cross section describes the absorption of energy within the particle. The extinction cross section, also called the total cross section, is given as the sum of both:

$$\sigma_{ext} = \sigma_{abs} + \sigma_{sca} \tag{12.1}$$

In case of the spherical particles, both of $\sigma_{sca,}$ and σ_{abs} are given by:

$$\sigma_{abs} = kIm[\alpha] = 4\pi k a^3 \times Im[g_d] \tag{12.2}$$

$$\sigma_{sca} = \left(k^4 / 6\pi\right) I\alpha I^2 = \left(8\pi / 3\right) k^4 a^6 I\, g_d I^2 \tag{12.3}$$

Where $\boldsymbol{k} = 2\pi / \lambda$, $\boldsymbol{\alpha}$ is the dipole polarizability that equal to $4\pi g_d a^3$, and $\boldsymbol{g_d}$ is the asymmetrical term for a dipole that equals to $\varepsilon_i - \varepsilon_m/\varepsilon_i + \chi\varepsilon_m$. In addition, χ is a shape-dependent parameter which equals to 2 for a sphere and can be larger (smaller) for other shape. This means that the extinction cross section (σ_{ext}) as a function of LSPR frequency could be given by:

$$\sigma_{ext}(\omega) = 9\frac{\omega}{c}\varepsilon_m^{3/2} V_0 \frac{\varepsilon_{i,2}(\omega)}{\left|\varepsilon_{i,1}(\omega) + 2\varepsilon_m\right|^2 + \varepsilon_{i,2}(\omega)^2} \tag{12.4}$$

Where V_0 is the volume of spherical shape that equal to $4\pi R^3/3$. The optical cross section against the actual physical geometrical cross section of the sphere, a dimensionless optical efficiency is used:

$$Q_{ext} = \frac{\sigma_{ext}}{\pi a^2}; Q_{abs} = \frac{\sigma_{abs}}{\pi a^2}; Q_{sca} = \frac{\sigma_{sca}}{\pi a^2} \tag{12.5}$$

This presents a problem in identifying small particles from a background with larger particle sizes. By changing the property of the LSPR of the metal nanoparticle, the optical efficiencies can be tuned and it is possible to achieve absorption efficiency larger than 1 (Nagel and Scarpulla 2010), i.e., more energy is being absorbed per unit area. This is beneficial for applications such as where the heat energy absorbed is used to convert to another useful energy form such as electricity for solar cell or water splitting.

Factors that Affect the Localized Surface Plasmon Resonance

The oscillation frequency of the surface plasmon band (SP) is determined by four factors: the density of electrons, the effective electron mass, the shape, and size of the charge distribution. The frequency and width of SPR depend on the size and shape of the metal nanoparticles as well as on the dielectric constant of the metal itself and the surrounding medium (Kreibig and Vollmer 1995; Link and El-Sayed 2003). The extreme sensitivity of LSPR to the particle size and shape makes it an attractive research subject because the resonance wavelength can be tuned to fit a specific wavelength of interest. The absorption and scattering cross section of the spherical particles is dependent on their size with scattering which becomes dominant as the size increases as shown in Fig. 12.2. For gold nanoparticles, it is found that diameter *D* is lower than 20 nm, and the absorption channel is dominant. As the size increases, the scattering becomes dominant (Tesler et al. 2011). Simulation based on the Mie theory and experiment results showed that increasing the size also causes red-shifting and broadening the LSPR spectrum due to phase retardation effects and presence of higher order mode. The strength and the distance of the induced electric field also increased when the particle gets larger (Hutter and Fendler 2004; Willets and Van Duyne 2007; Yeshchenko et al. 2012).

For an asymmetrical shaped particle, the effects of L-SPR become more complex. Some additional parameters to consider are the axis at which the size increases, and the direction and polarization of the incident light. For example, the SPR absorption in spherical Au and Ag NPs occurs at about 520 and 410 nm, respec-

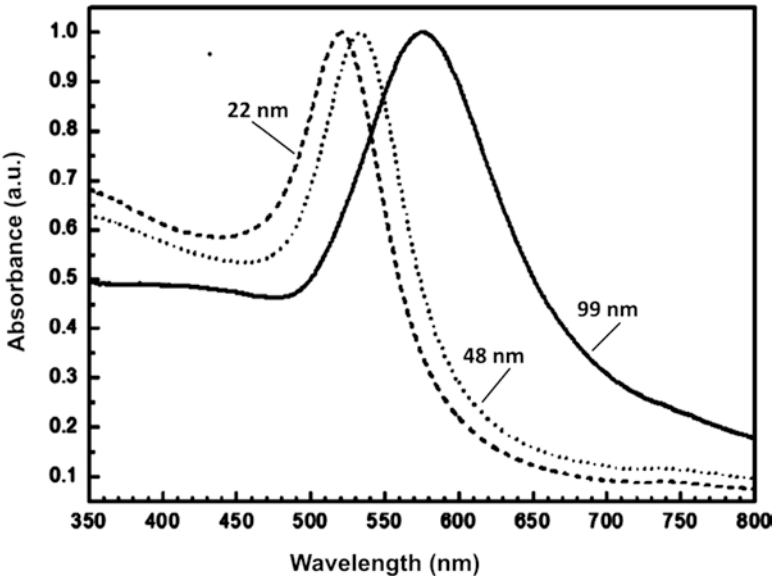

Fig. 12.2 Localized surface plasmon resonance (LSPR) of gold nanoparticles (Au NPs) dependent on the particle size. (Reprinted with a Copyright permission from Emam et al. 2017a)

tively (Fig. 12.3a). This absorption is absent for clusters (i.e., << 2 nm), as well as bulk Au. In the case of rod-shaped Au NPs, two absorption bands have been obtained (Emam et al. 2015). The first one which appears at ~ 520 nm corresponds to the oscillation of the electrons perpendicular to the long rod axis and is called transverse localized surface plasmon absorption (T-LSPR), which is insensitive to the nanorod length but coincides with the LSPR band of the spherical-like shapes (Emam et al. 2015; Henson et al. 2009). In addition, the second absorption band known as the longitudinal LSPR band that appears at a lower energy is caused by the oscillation of the free electrons along the long rod axis (Fig. 12.3b). Such band, the LSPR, is very sensitive to the aspect ratio (length/width) of the rods where a redshift occurs as the aspect ratio increases (Emam et al. 2015).

Other than the major change in the extinction spectrum across different shapes, a tremendous increase of electric field enhancement is found at the sharp edges. With this objective in mind, highly complex asymmetrical structures such as nanorice and nanostars deposition (Brand et al. 2006; Liu et al. 2013; Wu et al. 2009; Homan et al. 2011) are usually polycrystalline (Rodríguez-Oliveros and Sánchez-Gil 2012; Kumar et al. 2007) and become a subject of huge interest. For an example the LSPR band of triangular-shaped plasmonic nanoparticles split into three bands, longitudinal mode, transverse bands (i.e., in-plane dipole resonance

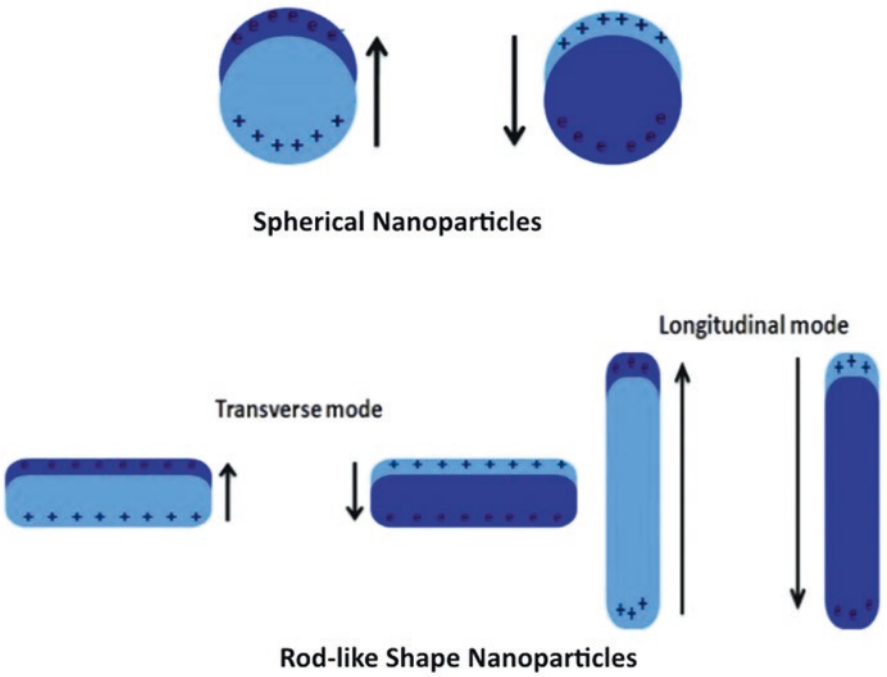

Fig. 12.3 Schematic representation of SPR excitation for spherical and rod-like shapes of gold nanoparticles. (Reprinted with a Copyright permission from Jayabal et al. 2015)

mode), and quadrupole bands (i.e., in-plane quadrupole and out-of-plane quadrupole resonances modes), as shown in Fig. 12.4 (Jin et al. 2001, 2003; Millstone et al. 2005; Callegari et al. 2003; Sherry et al. 2006). In such case, the maximum enhancement for the dipole resonance is at the tips. While for the quadrupole resonance, the regions for localized field enhancement are allocated at the sides. Afterward, the quadrupole band decayed away from the surface much faster than the dipole band around the particles tips, as shown in Fig. 12.4 (Kelly et al. 2003).

It is well-known that the dielectric constant of the surrounding media such as solvent or capping materials affects the SPR of metallic nanoparticles. Such an effect was attributed to the alteration in the ability of the surface to accommodate the electron density of the nanoparticles (Eustis and El-Sayed 2006; Jain et al. 2007). However, the capping material is the most important in determining the shift of the plasmon resonance. It is possible to shift away from the resonance peak from the interband transition by choosing an appropriate embedding medium. The dielectric constant of the surrounding medium determines the value ϵ and therefore the wavelength at which the resonance occurs. Medium with the higher dielectric function will cause further redshift to the resonance peak. Consequently, any chemically

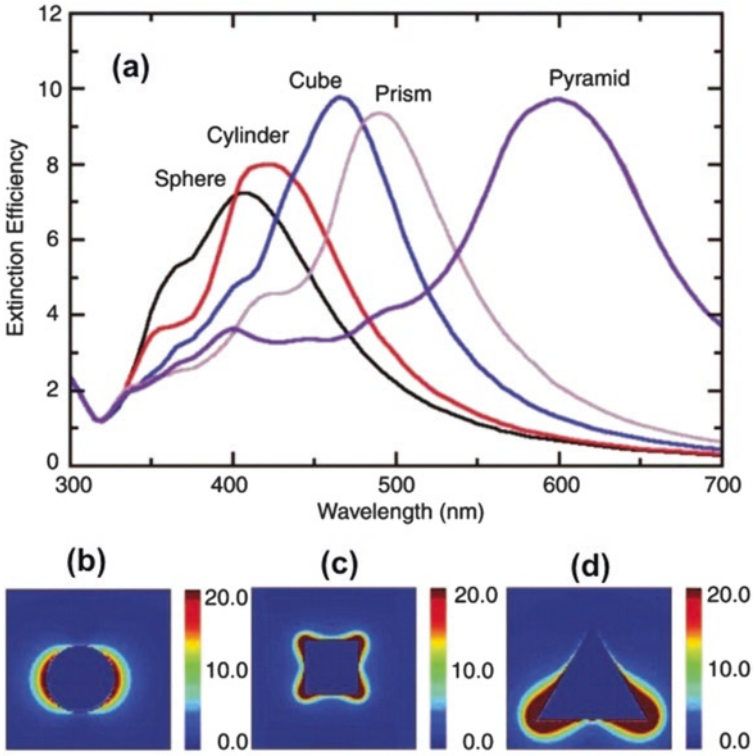

Fig. 12.4 (**a**) Extinction efficiency of silver nanoparticles in vacuum with same volume as of a 50-nm radius sized sphere but different shapes. The simulated electoral field contour map for corresponding (**b**) sphere, (**c**) cube, and (**d**) pyramid. (Reprinted with a copyright permission from Haes et al. 2005)

bonded molecules can detect the change in the electron density on the surface, which results in a change in the position of surface plasmon absorption band (Eustis and El-Sayed 2006). In metal nanoshell, the core material could be dielectric or semiconducting, whereas the shell material could be metallic nanoparticles. In these hybrid nanostructures, the SPR is strongly dependent on the relative thickness of the nanoparticle core and its metallic shell. Therefore, the position of the plasmon band can be tuned anywhere across the visible or infrared regions of the optical spectrum, by varying the core and shell thicknesses as shown in Fig. 12.5 (Jain et al. 2007; Oldenburg et al. 1998; Yu et al. 2017; Prodan et al. 2003; Jain et al. 2008; Ghosh Chaudhuri and Paria 2011).

Whereas, in the case of alloyed nanostructures, the position of the SPR absorption band is linearly dependent on their chemical composition (Link et al. 1999). Therefore, a strong redshift SPR band could be observed upon mixing of plasmonic nanostructures with other materials (e.g., magnetic or semiconducting materials) within the same nanoobject (Ghosh Chaudhuri and Paria 2011; Shi et al. 2006; Lee and El-Sayed 2006; Barcaro et al. 2015; Ferrando et al. 2008). As reported by Girgis et al. and Emam et al., this redshift in Au-Co compared to pure gold nanoparticles is due to the homogeneous mixture of the metal-metal bond between the alloys and constitutes such as gold and cobalt leading to the formation of an intermetallic or alloyed structure. In this case, Co^{2+} ions were diffused into the gold nanoparticles host crystal (Girgis et al. 2012), as shown in Fig. 12.6. Consequently, the alteration in the SPR for the host crystal gold nanoparticles via electronic charging or loss of

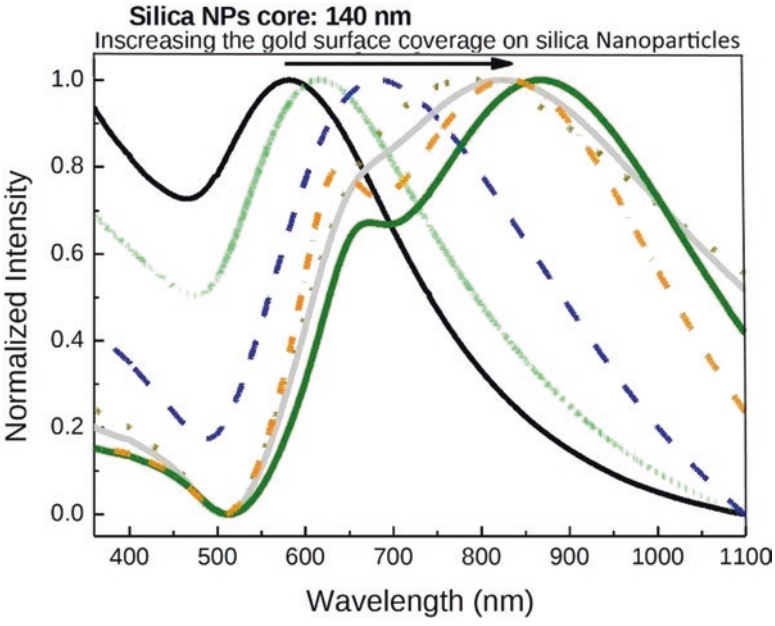

Fig. 12.5 Redshift in the absorption spectra of silica-gold core-shell nanoparticles with increasing in the gold nanoshells on silica nanoparticles. (Reprinted with permission from Lien et al. 2014)

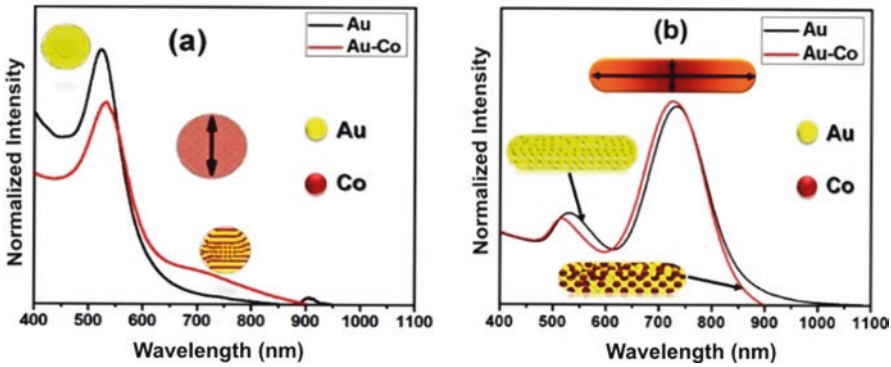

Fig. 12.6 (**a**) Redshift surface plasmon absorption band in case of spherical gold-cobalt nanoalloys compared to pure gold nanoparticles (**b**) Blue shift in the surface plasmon absorption band in case of rod-like shape of gold-cobalt alloyed nanoparticles. (Reproduced with permission from Emam et al. 2015)

continuous density of states causing a plasmon band shift (Emam et al. 2015; Xu et al. 2007; Boyer et al. 2010).

12.3 Metal-Enhanced Fluorescence

The fluorescence emission of fluorophores can be enhanced by attaching them to materials that exhibit plasmon resonance, commonly known as metal-enhanced fluorescence (MEF) (Geddes 2010, 2013; Geddes and Lakowicz 2002; Xie et al. 2006; Deng et al. 2013). This is also sometimes referred to as plasmon-enhanced fluorescence (PEF) (Bauch et al. 2014; Gandra et al. 2014; Feng et al. 2015). In MEF, the emission is enhanced owing to a strong localized field enhancement that is near the metal surface because the surface plasmons are being excited by the light. Through the interaction of the fluorophore molecule with the metal surface, decay rates for the fluorophore are altered which leads to fluorescence enhancement (Morton et al. 2011). The strength of the MEF depends mainly on spectra overlapping of the excitation and emission of the fluorophores to the plasmon resonance wavelength of the metal (Geddes 2010; Chen et al. 2007; Bharadwaj and Novotny 2007; Emam et al. 2017b), location of hot spots (Yuan et al. 2013), and the metal-fluorophore distance (Gandra et al. 2014; Emam et al. 2017b; Zhou et al. 2014; Mishra et al. 2013).

There are two main processes that give rise to MEF: First of them is the external E-field that influences the molecules and the second one is based on the emission of radiation influenced by local field environment. When a fluorophore is in the vicinity of a plasmon resonating nanoparticle, the fluorophore will experience the E-field generated by the nanoparticle. Those enhanced electric fields increase the amount of energy absorbed by the fluorophore known as excitation enhancement. The rate of

the enhanced excitation field (E_{ex}) can be expressed into the following relationship:

$$E_{Ex} = \frac{\left|\boldsymbol{E}\left(x_d, \lambda_{ex}\right) \cdot \boldsymbol{p}\right|^2}{\left|E_i\right|^2} \tag{12.6}$$

Where (x_d, λ_{ex}) is the electric field at the position and wavelength of excitation, ŭ5D; is the emitters (fluorophore in this case) orientation, and E_i is the incident free space electric field without the presence of nanospheres. In MEF, the electromagnetic coupling between the fluorophore and the nanoparticle plasmon also causes an increase in the radiative decay rate of the molecule at the emission wavelength or decreases the decay rate if quenching occurs. This emission enhancement introduces new radiative and non-radiative decay rates (Γ_m *and* $\Gamma_{m,nr}$), and modifies both the quantum yield and lifetime of the fluorophore as follow:

$$Q_0 = \frac{\Gamma_0}{\left(\Gamma_0 + k_{nr}\right)} \leftrightarrow Q_m = \frac{\left(\Gamma_{nr} + \Gamma_{0,r}\right)}{\left(\Gamma_{m,r} + \Gamma_{0,r} + \Gamma_{m,nr} + k_{nr}\right)} \tag{12.7}$$

$$\tau_0 = \frac{1}{\left(\Gamma_r + k_{nr}\right)} = \frac{Q_0}{\Gamma} \leftrightarrow \tau_m = \frac{1}{\left(\Gamma_{m,r} + \Gamma_{0,r} + \Gamma_{m,nr} + k_{nr}\right)} \tag{12.8}$$

Where Q_m is the modified quantum yield due to MEF, the subscript ŭ5A; represents a modified term due to the plasmon coupling. The ability to modify the quantum yield of the fluorophores is an important benefit for MEF because fluorophores with poor quantum yields can be improved externally through coupling with SPR generated by the metal (see Fig. 12.7).

In such case, the final emission will be enhanced, which is given by:

$$E_m = \frac{Q_m}{Q_0} \tag{12.9}$$

Together, the new excitation and decay rate increased the rate of total fluorescence emission (E_F), and is related by the following relationship:

$$E_F = E_{Ex} E_{Em} \tag{12.10}$$

It is worth emphasizing that from the above equations, the MEF is primarily due to (1) E-field enhancement which boosts the excitation rate of the fluorophores, and (2) the addition of new radiative decay channels that improve the emission rates and quantum yields. In the case where the fluorophore has an intrinsic high quantum yield, the emission enhancement will not be significant. Several parameters and criteria must be taken into consideration to be useful in the fabrication and engineering of metal-enhanced fluorescence-based hybrid nanocomposites. These parameters include *(i)* the degree of spectral overlaps between the emission spectra of the fluorophore and

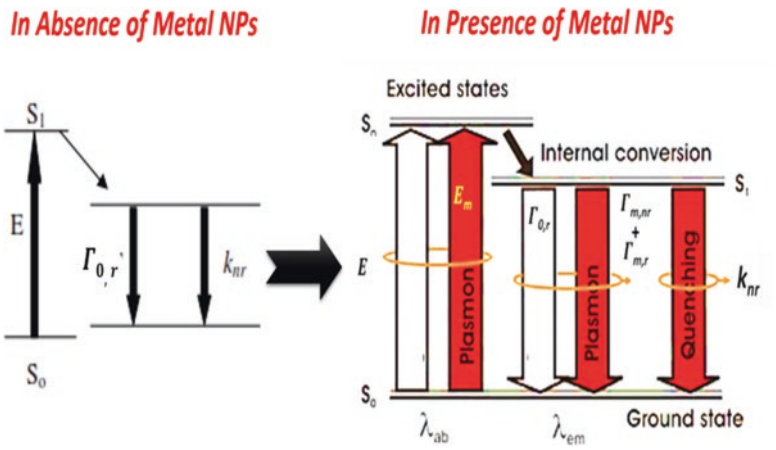

Fig. 12.7 A simplified Jablonski diagram showing the additional decay routes in both of presence and absence of plasmonics nanostructures. (Adopted from Bauch et al. 2014)

LSPR spectra (Geddes 2010; Chen et al. 2007; Lakowicz 2005) and *(ii)* the fluorophores should all be located at region of "hot spots" where electric field generated by SPR is the highest (Aslan et al. 2005; Yuan et al. 2013; Hrelescu et al. 2011; Fales et al. 2011). Finally, metal-fluorophore distance is widely recognized that the MEF is highly dependent on the distance between the fluorophores and the metal nanoparticles. Quenching occurs when the fluorophores are too close to the metal and facilitate non-radiative energy transfer and dissipation of energy in the fluorophore-metal system (Gandra et al. 2014; Zhou et al. 2014; Mishra et al. 2013; Ray et al. 2006a; Dragan et al. 2012), (See Fig. 12.8). At distance below the optimum enhancement, the enhancement factor follows a ŭ5F;$^{-6}$. Whereas when the distance gets further away, the dipole near-field of the SPR drops ∝ 1/ŭ5F;^{3} (or $1/r^5$ for quadrupole) and thus weakened the enhancement (Zhou et al. 2014; Chatterjee et al. 2011). However, an optimum distance appears to depend on the surrounding medium and the plasmonic structures (Eustis and El-Sayed 2006; Zhou et al. 2014; Chatterjee et al. 2011; Dulkeith et al. 2005). For example, Li et al. demonstrated that the magnitude of the fluorescence enhancement in C-dots/Ag@SiO_2 hybrid nanocomposites increases as a function of metal-fluorophore distance by the adjusting of the silica spacer thickness (Li et al. 2012).

12.4 Engineered Hybrid Nanocomposites for MEF Effect

Since the discovery of metal-enhanced fluorescence (MEF), it has been receiving huge attention and soon becomes a very active research field. Leading by recent technology push from advancement in nanofabrication and characterization techniques, various fabrication techniques, materials, and structures have been explored progressively to obtain better MEF structures. Gold and silver are the primary candidates of interest due to their SPR in visible and NIR regions. Regardless, both metals can offer large

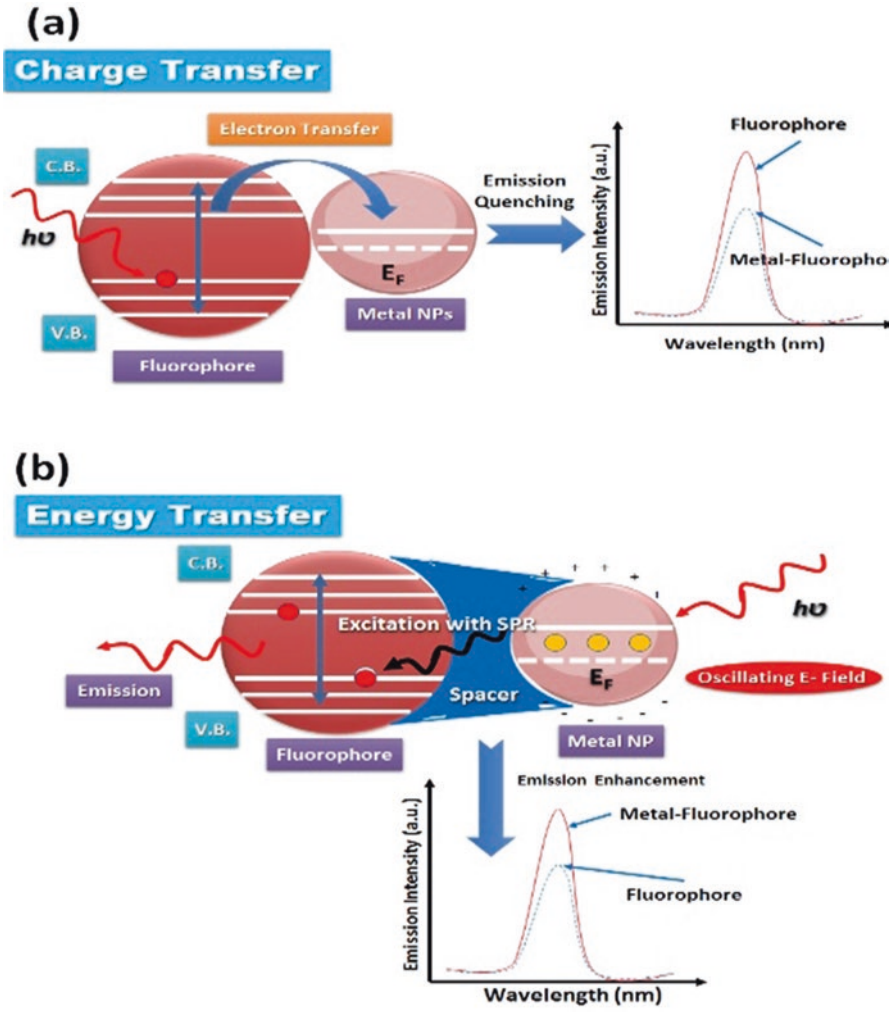

Fig. 12.8 A simplified schematic diagram shows the possible plasmonic enhanced fluorescence mechanisms (**a**) Quenching and (**b**) Enhancement

enhancement factors, and the signal is usually homogeneous throughout the substrate, which is important for biosensing and bioimaging applications (Deng et al. 2013).

In this section, an overview of the achieved work was done by our research group and others regarding using of engineered hybrid nanocomposites to achieve MEF mechanism. First of these studies is that achieved by Ragab et al. (Gadallah et al. 2013). They investigated the plasmonics effects of Ag NPs on the collective optical properties of fluorescein dye at different v/v ratios. In such study, a remarkable enhancement in the absorption and emission of fluorescein dye with an enhancement factor about threefold has been detected, as shown in Fig. 12.9. In addition, a significant increase in the rate of radiative decays was detected (Gadallah et al. 2013). These obtained enhancement mechanisms are attributed to a modification of

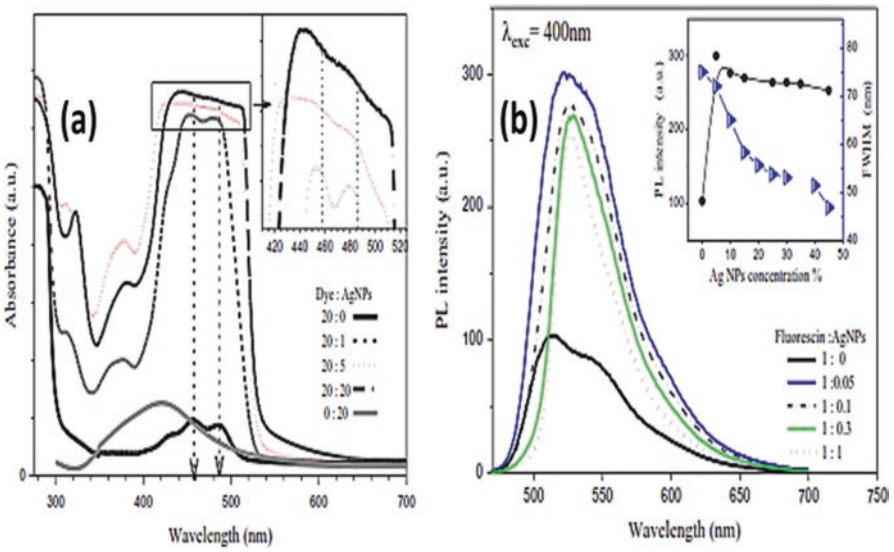

Fig. 12.9 (**a**) Absorption and (**b**) emission spectra of fluorescein dye, silver nanoparticles, and fluorescein: silver nanoparticles mixtures. (Reprinted with a copyright permission from Gadallah et al. 2013)

the local density of EM-modes in the vicinity of Ag nanoparticles at energies resonant with surface Plasmon (Xu et al. 2004).

In other studies, the influence of plasmonic nanostructures such as Au and Ag NPs has been investigated on the photo-physical properties of the semiconductor quantum dots such as CdSe and CdTe nanocrystals (Ragab et al. 2014a, b; Giba et al. 2015; Rady 2018). Ragab and co-workers demonstrated the influence of plasmonic silver nanostructures on the photo-physical properties especially the emissive (i.e., steady-state and upconversion) and laser spectroscopic properties of CdTe NCs (Ragab et al. 2014a, b; Giba et al. 2015). They reported in their studies a remarkable enhancement in the emission efficiencies upon the addition of Ag NPs at different CdTe:Ag NPs v/v ratios up to 11-fold, followed by a reduction in the radiative lifetimes (see Fig. 12.10) (Ragab et al. 2014a). This enhancement effect was attributed to energy transfer between the resonant (coupling) plasmonic field of Ag NPs and CdTe excitonic energy state. Although, no significant change in the upconversion spectrum either in the presence or absence of Ag NPs; an increase in both the absorption and emission rate of CdTe QDs was noticed.

Furthermore, Mansour *et al.* developed chemically a type of Plasmonic/Semiconductor such as Au/CdSe heterostructures of controlled morphology and their hybrid nanocomposites with graphene (Rady 2018; Mansour et al. 2017). Based on the photo-physical measurements, the presence of plasmonic nanocrystals such as Au NPs in direct contact with the semiconductor quantum dots such as CdSe QDs could enhance the optical absorptivity but quench their photoluminescence properties due to the charge transfer from the conduction band of the semiconductor to the Fermi level of the metallic part as shown in Fig. 12.11 (Mansour et al. 2017; Hsieh et al. 2007; Pons et al. 2007).

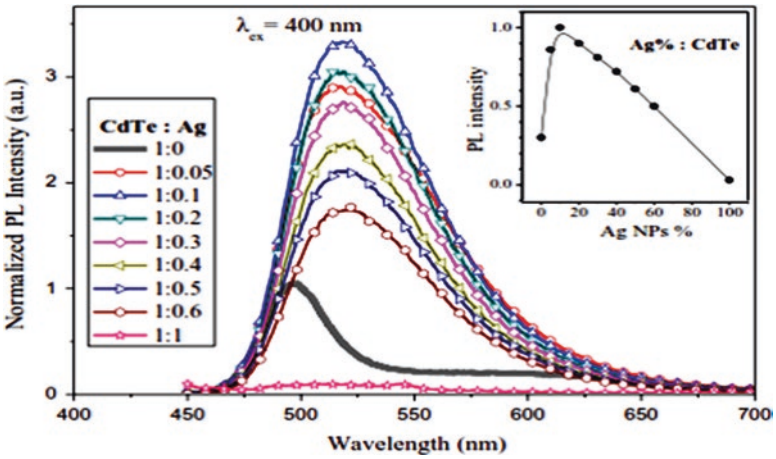

Fig. 12.10 PL of CdTe:Ag nanohybrids at different concentrations of Ag nanoparticles. (Reprinted with a copyright permission from Ragab et al. 2014a)

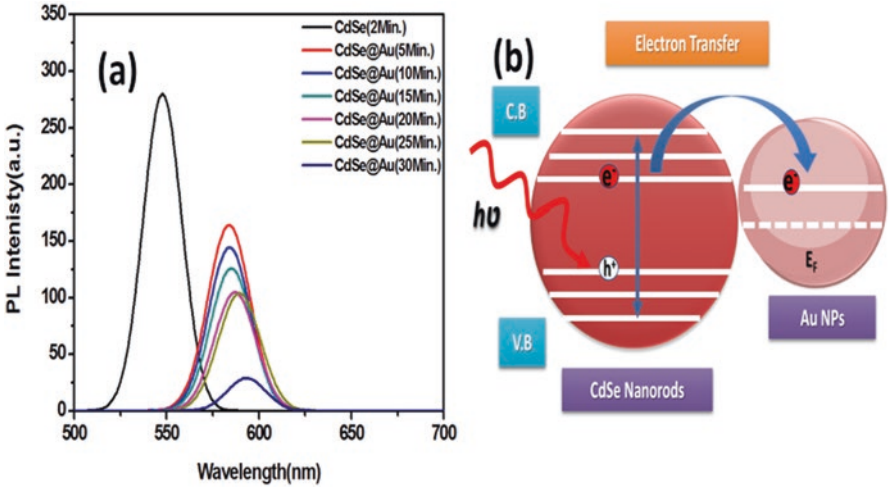

Fig. 12.11 (**a**) PLE spectra of Au/CdSe tetrapod-like shape heterostructure, (**b**) fluorescence quenching mechanism in Au/CdSe. (Reused from Rady 2018)

In contrast, besides the increase in the optical absorptivity, a remarkable enhancement of the quantum efficiency has been observed for the Au/CdSe heterostructures in presence of graphene (about ~ 4.5 to 12 fold intensity in the emission intensity) as shown in Fig. 12.12. This might be because the rate of the electron transfer from graphene to the metal is faster than that from semiconductor to the metal achieving the MEF effect in hybrid nanostructures based on metal/semiconductor heterostructures such as Au/CdSe tetrapods (see Fig. 12.13) (Rady 2018).

Finally, Emam et al. developed a novel fluorescent hybrid nanocomposite as an alternative to plasmonic/cadmium-based quantum dots such as plasmonic/C-dots. These hybrid nanocomposites include C-dots/Au and C-dots/Ag nanohybrids that

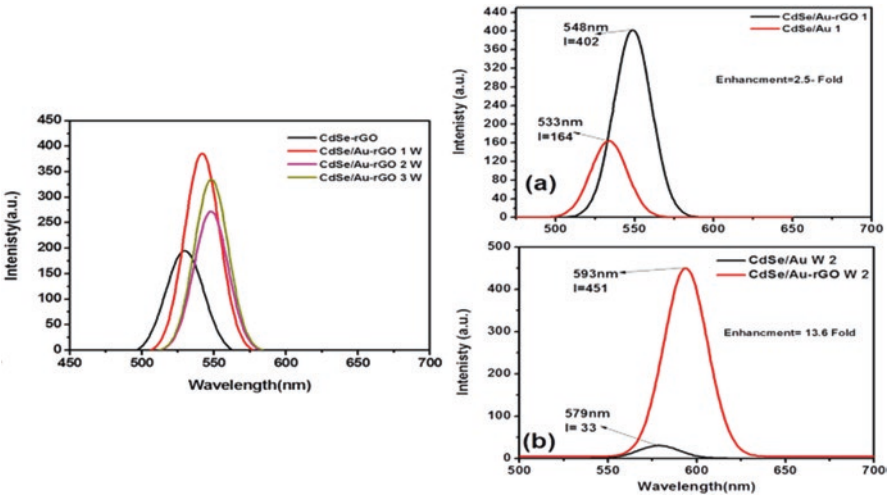

Fig. 12.12 PLE spectra of Au/CdSe tetrapod-like shape heterostructure in presence of rGO. (Reused from Rady 2018)

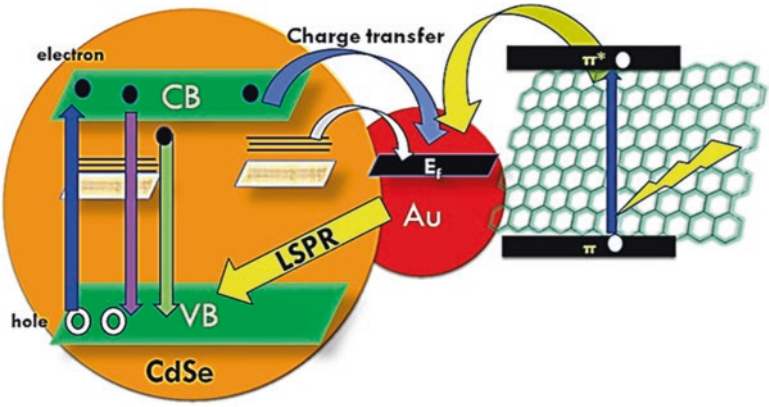

Fig. 12.13 Schematic diagram for PLE enhancement mechanism in Au/CdSe tetrapod heterostructure upon their loading on rGO. (Reused from Rady 2018)

are chemically prepared via microwave irradiation (MWI) method (Emam et al. 2017b; 2018). Remarkable enhancements in the collective optical properties and parameters such as absorptivity and fluorescence quantum yield (FL-QY), accompanied with the reduction in the rate of electron-hole recombination were observed for the hybrid nanostructure compared to pure C-dots (Emam et al. 2017b; 2018) as shown in Figs. 12.14 and 12.15 and Table 12.1.

This enhancement is due to enhancing the incident excitation field via L-SPR in metallic part, which leads to increasing the exciton radiative recombination rate in the carbon dots, which is dependent on the spectral overlap in the absorption spectra.

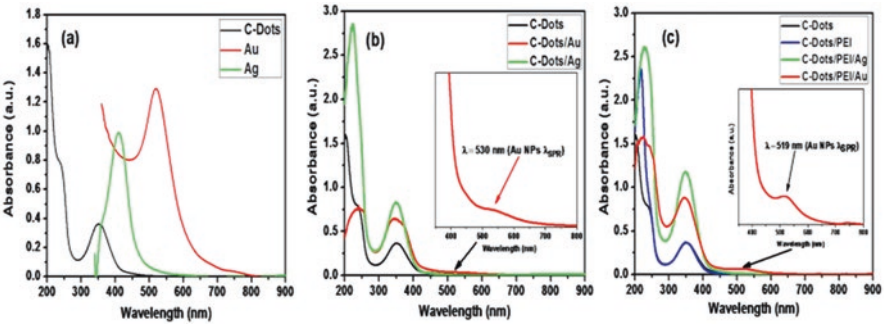

Fig. 12.14 Absorption spectra for each of (**a**) naked C-dots, Ag, and Au NPs, respectively. (**b**) C-dots, C-dots/Ag, and C-dots/Au nanohybrid, and (**c**) naked C-dots, C-dots/PEI, C-dots/PEI/Ag, and C-dots/PEI/Au nanohybrids. (Reprinted with a copyright permission from Emam et al. 2017b)

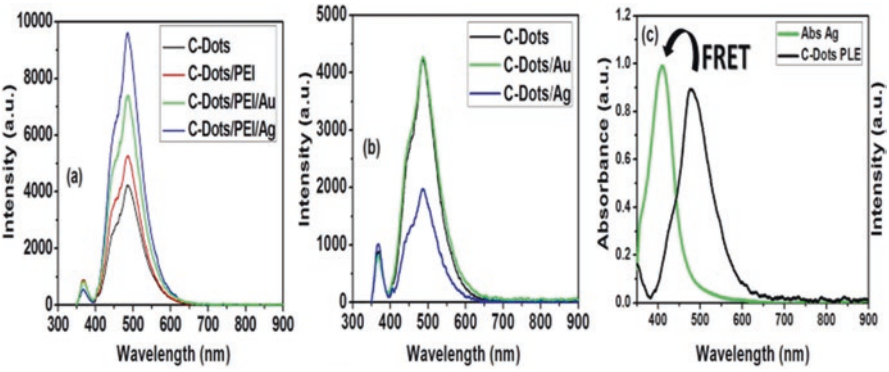

Fig. 12.15 Effect of plasmonic NPs on the PLE features of C-dots; (**a**) in the presence or (**b**) in the absence of spacer (i.e., PEI) upon excitation at steady-state condition (i.e., 366 nm). (**c**) Spectral overlapping between PLE spectra C-dots (black line) and the adsorption spectrum of Ag NPs (green line). (Reprinted with a copyright permission from Emam et al. 2017b)

Table 12.1 Influence of plasmonic nanoparticles (Au and Ag NPs) on the PLE properties of C-dots in presence or absence of polymeric spacer (i.e., PEI) (Emam et al. 2017b)

	At λ_{ex} [(a)] 366 nm			
Sample	I[(b)]	I/I_0[(c)]	QY/QY_{Dye} [(d)] (steady-state)	FWHM [(e)] (steady-state)
C-dots	(I_0) 4223.69	–	22.468	33.60484
C-dots/Au	4683.54	1.11	36.40	86.74477
C-dots/PEI/Au	7403.64	1.75	55.52	30.56937
C-dots/Ag	1833.45	0.434	8.723	2.5756916
C-dots/PEI/Ag	9134.23	2.16	77.213	17.44447

Reprinted with a copyright permission from Emam et al. (2017b)
[(a)]**λ_{ex}:** excitation wavelength. [(b)]**λ_{em}:** PLE wavelength. [(c)]**I/I_0:** relative enhancement factor. [(d)]**QY/QY_{Dye}:** relative quantum yield. [(e)]**FWHM:** full width at half-maximum

This plasmonic enhancement was more pronounced in the case of C-dots/Ag than that of C-dots/Au nanohybrids, due to low intrinsic loss and the degree of the overlap between the absorption spectra of AgNPs and C-dots. Furthermore, picosecond decay measurements show a decreased lifetime of C-dots in the presence of the plasmonic effect, due to the increased rates of radiative decay (see Fig. 12.16).

As shown in Fig. 12.17, the possible interactions between plasmonic material and fluorophores could be summarized as follows: (i) the excitation field can be enhanced through a coupling between the surface plasmon (SP)-assisted generated local field into the incident field. In such a case, plasmonic nanostructure could act as an optical concentrator for the incident source, resulting in a remarkable enhancement of optical absorption; furthermore, (ii) plasmonic nanostructures could be used as an excitation source to excite the fluorophore, as long as their SP energy is much higher than the band-gap emission of fluorophores (Achermann 2010; Sun et al. 2009; Hwang et al. 2009). Finally, iii) conversely to the previous pathway, PLE could be enhanced via an efficient energy transfer between the fluorophores and the plasmonic nanostructures when the exciton energy is greater than SP energy, which attributed to exciton-SP quadrupole interaction (Achermann 2010; Zhou et al. 2011; Cheng et al. 2010). Depending on the band structures of fluorophores (i.e. HOMO & LUMO) and plasmonic particles (i.e. Fermi level & Wave function), the PLE quenching or enhancement could be achieved (Deng et al. 2013; Achermann 2010; Sun et al. 2009; Hwang et al. 2009; Shevchenko et al. 2008; AbouZeid et al. 2011; Liaw et al. 2014; Zhang et al. 2007). If the C-dots based on fluorophores are located in a close proximity to the metallic surface, a non-radiative dumping is due to either energy transfer between the C-dots and the metal or the electron transfer from C-dots to the metal (Fig. 12.17a) (Emam et al. 2017b, 2018). Whereas the C-dots/

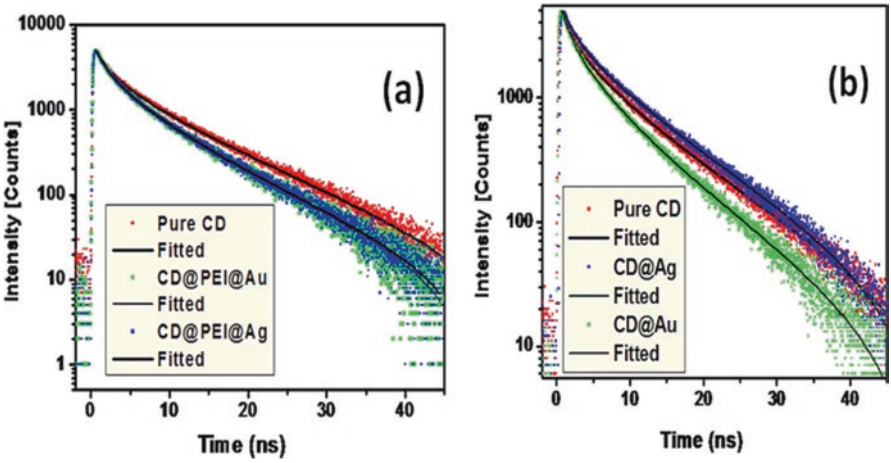

Fig. 12.16 Effect of plasmonic nanostructures (i.e., Ag and Au) on the radiative decay of the C-dots in presence (**a**) and absence (**b**) of dielectric polymeric spacer. (Reprinted with a copyright permission from Emam et al. 2018)

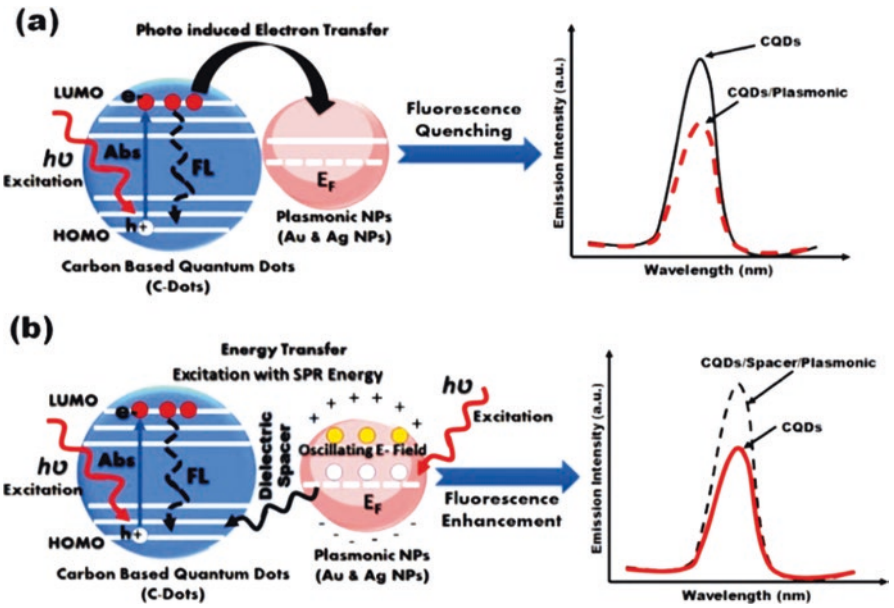

Fig. 12.17 Schematic diagram for (**a**) enhancement and (**b**) quenching mechanism C-dots/plasmonic. (Reprinted with a copyright permission from Emam et al. 2017b)

plasmonic hybrid nanostructures are separated with a dielectric spacer such as polymer (i.e., distance increase), light–mater interactions will be enhanced near the metal surface based on the enhancement of local fields associated with the SP of the metallic part. This effect could enhance the fluorescence of the C-dots based on fluorophore part as significantly shown in Fig. 12.17b (Hsieh et al. 2007; Pons et al. 2007; Ran et al. 2014).

12.5 Biomedical Applications of Engineered Metal-Enhanced Fluorescence Nanosystems

12.5.1 Biosensing

During the last decade, metal-enhanced fluorescence (MEF)-based engineered hybrid nanocomposites have been used in the fabrication of biosensor nanosystems to improve the sensitivity of fluorescence detection to detect molecules/moieties (Lee et al. 2011; Xu et al. 2017; Jeong et al. 2018) and heavy metals (Peng et al. 2018) at ultra-low concentrations. Along with signal enhancement, this promising technology allows advanced biological analysis for specified biomarkers and bioimaging on an adequate design.

As previously mentioned above, the MEF process depends on several critical parameters to induce desirable effects, consequently introducing a new trend in fluorescence detection. Therefore, it is essential to use brighter and more photostable fluorophores to achieve a high level of sensitivity of the biosensor. In MEF-based biosensors, the presence of metal near the fluorophore increases the rate of excitation and emission by opening additional electron configurations of fluorophores. In addition, it increases the photostability and emissive properties (i.e. fluorescence quantum yield, FLQY) of fluorophores compared to other conventional fluorophore-based biosensor (Feng et al. 2015; Emam et al. 2017b; Li et al. 2012; Emam et al. 2018; Khurgin et al. 2007; Lakowicz et al. 2008; Ray et al. 2006b). Furthermore, MEF-nanosystems provide an advantageous method for fabrication of biosensing platform. Such platform that can combine between the sensing transducers fluorophores and a plasmonic-based amplifier for the resultant signal within a single system, compared to traditional biosensors (see Fig. 12.18). Thus, these features explain why MEF is beneficial for fluorescence-based detection, and the robust platform based on MEF is a promising tool for producing effective biosensors (Jeong et al. 2018).

Mei and Tang developed a biosensor based on multilayered hybrid nanocomposites for DNA detection using layer-by-layer (LbL) deposition technique. In such configuration, a layer of colloidal gold nanorods (AuNRs) was deposited on a glass substrate via solvent evaporation to be used as a nano-antenna for DNA detection and propagate the L-SPR for achieving MEF effect (Jeong et al. 2018; Mei and Tang 2016). Then another layer of fluorophore materials (i.e., dye) was loaded onto the AuNRs layers (see Fig. 12.20). A remarkable enhancement in the fluorescence intensity upon the attachment of DNA onto the AuNRs array chip as analyst is due to the MEF effect (Mei and Tang 2016).

In other configuration, which developed by Feng *et al.* based on using of functional materials such as polyelectrolyte to be a building block for fabrication of multilayered MEF-based biosensor. In such configuration, a layer of plasmonic nanostructures (i.e. AuNRs) was deposited onto a glass substrate using LbL technique, followed by loading of upconversion nanoparticles (i.e. lanthanide-doped NPs) as fluorophores. To achieve the MEF phenomena, the plasmonic AuNRs were separated from fluorescent lanthanide-doped NPs via deposition polyelectrolyte as a dielectric spacer as shown in Fig. 12.19b (Feng et al. 2015). Feng et al. reported that by modulation of the aspect ratio of AuNRs, the LSPR wavelength within the NIR region ~ 980 nm matches with the excitation wavelength of upconverted nanoparticles resulting in a remarkable fluorescence enhancement up to 22.6-fold with 8-nm spacer thickness. This proposed MEF-based biosensor configuration was a unique platform for bioimaging applications (Feng et al. 2015).

Moreover, a new type of biosensing platform, MEF-based biosensor, is developed by Ji and co-worker (Ji et al. 2016). In this biosensing system, Ag zigzag nanorod arrays were formed via LbL techniques using oblique angle deposition (see Fig. 12.19c) and were studied to determine whether it is suitable for MEF applications. By changing the fold number—the morphology of the Ag zigzag shape—a 14-fold and 28-fold enhancement factor is achieved for biotin-neutravidin, and the hybridization of two single-stranded oligonucleotides with 33-base detection was obtained (Ji et al. 2016). In addition, the limit of sensitivity was increased to 0.1 pM of targeted analyte.

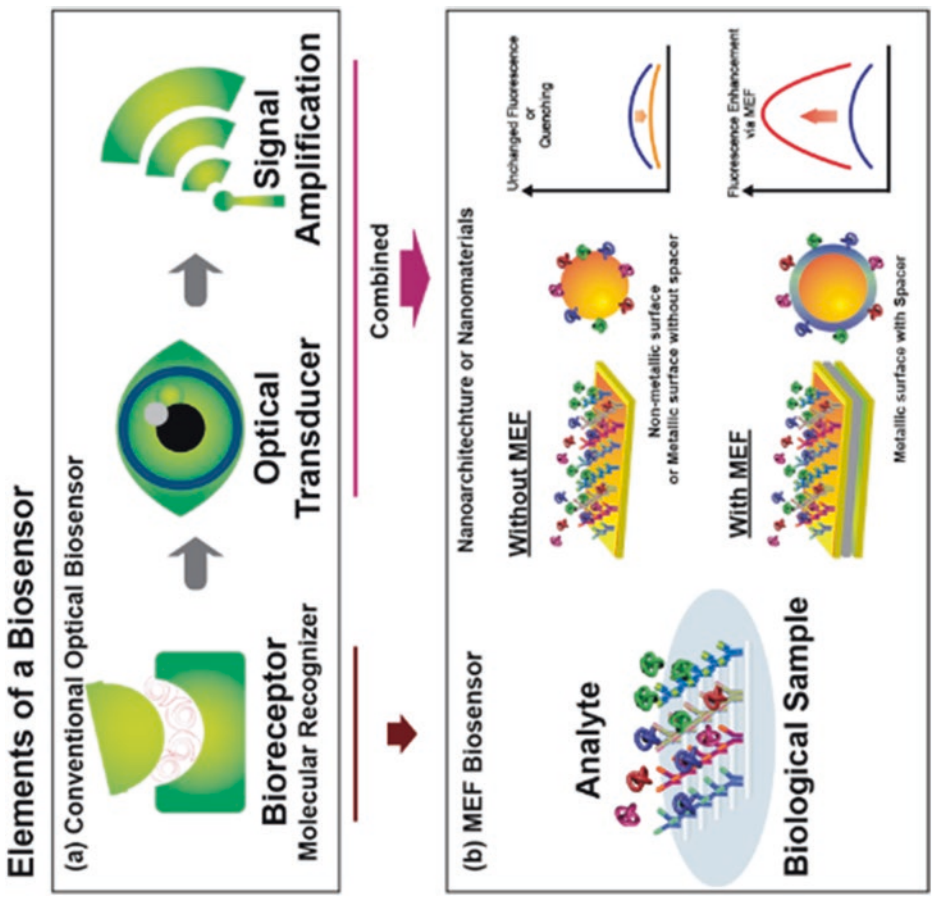

Fig. 12.18 The concept of optical biosensors, (**a**) conventional optical biosensor and (**b**) its correlation to MEF platforms for optical biosensors. (Reprinted with a copyright permission from Jeong et al. 2018)

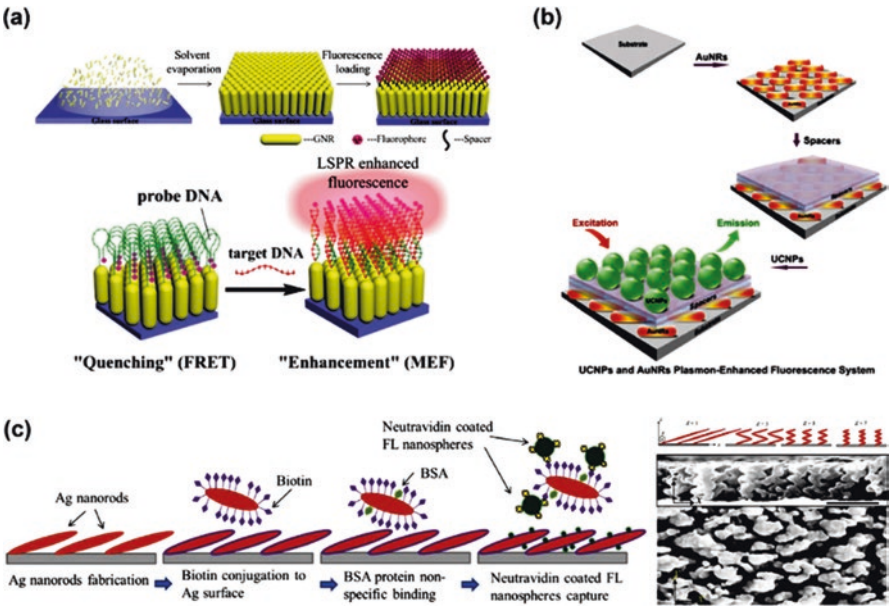

Fig. 12.19 Schematic diagram for fabrication MEF control via layer-by-layer (LbL) deposition. (**a**) The ordered gold nanorod (GNR) array chip for DNA detection upon hybridization. (**b**) Fluorescence enhancement of upconversion NPs (UCNPs) using polyelectrolyte multilayer deposition. (**c**) MEF of zigzag Ag nanorod arrays. (Reprinted with a copyright permission from Jeong et al. 2018, Mei and Tang 2016, Feng et al. 2015, Ji et al. 2016)

In other applications of biosensing, nanosystem based on detection of contaminants such as heavy metal (i.e., Pb^{2+}, Cd^{2+}, Cu^{2+}, Zn^{2+}, and Cr^{3+} etc.…) has been demonstrated by Peng and co-workers (Peng et al. 2018). In such study, silica nanoparticles (SiO_2) are used to enhance the fluorescence properties of SGT1-SGT3 dyes and improve the detection sensitivity limits of SGTs-SiO_2 for heavy metal ions up to 1.81 and 0.0532 nM for Hg^{2+}, and Cd^{2+}, respectively.

Finally, Emam et al. developed a novel fluorescent and less toxic hybrid nanocomposites based on plasmonic/C-dots such as C-dots/PEI/Au and C-dots/PEI/Ag nanohybrids. These hybrid nanocomposites are prepared via chemical routes based on microwave irradiation method and physical conjugation of plasmonic nanostructures to PEI-coated C-dots (Emam et al. 2017b, 2018). A remarkable enhancement in the collective photo-physical properties (i.e., molar absorptivity and fluorescence quantum yield (FL-QY)). In addition, their approach allows the fabrication of engineered multi-modal hybrid nanocomposites based on MEF mechanism to be used in a wide range of applications such as chemical/biological sensing, probing, and theranostics (i.e. therapy and imaging), as shown in Fig. 12.20 (Emam et al. 2017b).

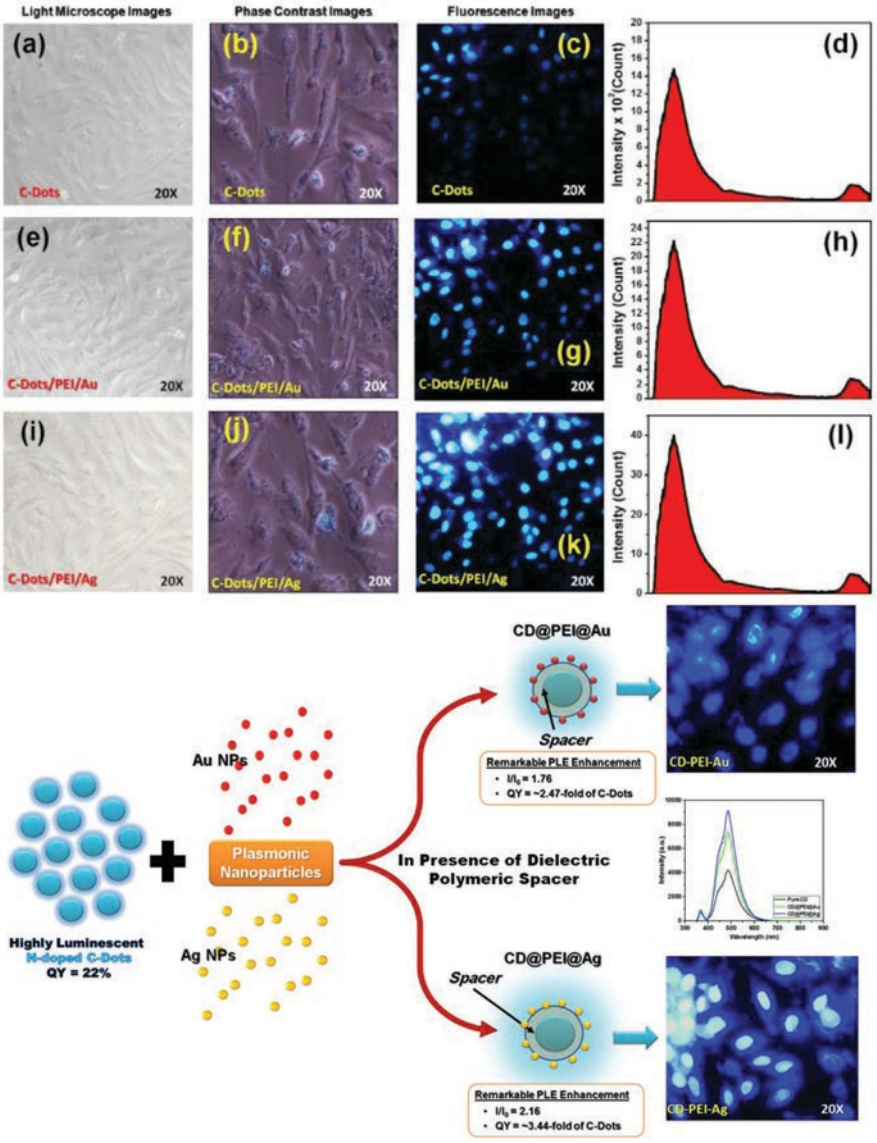

Fig. 12.20 Bright field (**a**, **e**, and **i**), phase contrast (**b**, **f**, and **j**), and fluorescence images (**c**, **g**, and **k**) of HepG-2 cells after 24-h incubation, and the intensity histogram (**d**, **h**, and **l**) of fluorescence images. (**a**, **b**, and **c**) for C-dots. (**e**, **f**, and **g**) for C-dots/PEI/Au nanohybrids. (**i**, **j**, and **k**) for C-dots/PEI/Ag nanohybrids. (Reprinted with a copyright permission from Emam et al. 2017b)

12.6 Conclusion

In conclusion, we introduced an overview about the optical properties of plasmonic nanomaterials and the parameters that affect the strength of the localized surface plasmon resonance (L-SPR), in addition to the required criteria to achieve successful metal-enhanced fluorescence (MEF) effect. Furthermore, in this chapter, we introduce a survey about our recent research works which was done regarding use of engineered hybrid nanocomposites to achieve MEF mechanism that opens new doors for multi-functional materials in so many applications such as chemical analysis, biosensing, biomedical imaging, and early diagnosis of cancers.

Acknowledgments The authors gratefully appreciate the Science and Technology Development Fund (STDF) for providing financial support through Grant ID: 6066, entitled "Novel Hybrid Carbon based Nanocomposites for Biosensors and Biomedical Imaging Applications", and grant ID: 1719, "Plasmonic-Semiconductor hybrid Nano-structural Solar Cells: toward Low Cost Great Enhancement of Solar Cell Efficiency".

References

AbouZeid KM, Mohamed MB, El-Shall MS (2011) Hybrid Au–CdSe and Ag–CdSe nanoflowers and core–shell nanocrystals via one-pot heterogeneous nucleation and growth. Small 7:3299–3307. https://doi.org/10.1002/smll.201100688

Achermann M (2010) Exciton− plasmon interactions in metal− semiconductor nanostructures. The Journal of Physical Chemistry Letters 1:2837–2843. https://doi.org/10.1021/jz101102e

Aslan K, Lakowicz JR, Geddes CD (2005) Rapid deposition of triangular silver nanoplates on planar surfaces: application to metal-enhanced fluorescence. J Phys Chem B 109:6247–6251. https://doi.org/10.1021/jp044235z

Barcaro G, Sementa L, Fortunelli A, Stener M (2015) Optical properties of nanoalloys. Phys Chem Chem Phys 17:27952–27967. https://doi.org/10.1039/C5CP00498E

Bardhan R, Grady NK, Cole JR, Joshi A, Halas NJ (2009) Fluorescence enhancement by Au nanostructures: nanoshells and nanorods. ACS Nano 3:744–752. https://doi.org/10.1021/nn900001q

Bauch M, Toma K, Toma M, Zhang Q, Dostalek J (2014) Plasmon-enhanced fluorescence biosensors: a review. Plasmonics 9:781–799. https://doi.org/10.1007/s11468-013-9660-5

Bharadwaj P, Novotny L (2007) Spectral dependence of single molecule fluorescence enhancement. Opt Express 15:14266–14274. https://doi.org/10.1364/OE.15.014266

Boyer P, Ménard D, Meunier M (2010) Nanoclustered Co− Au particles fabricated by femtosecond laser fragmentation in liquids. J Phys Chem C 114:13497–13500. https://doi.org/10.1021/jp1037552

Brand WH, Daniel W, Le F, Nordlander P (2006) Halas Naomi. J Nano Lett 6:827–832. https://doi.org/10.1021/nl060209w

Callegari A, Tonti D, Chergui M (2003) Photochemically grown silver nanoparticles with wavelength-controlled size and shape. Nano Lett 3:1565–1568. https://doi.org/10.1021/nl034757a

Chatterjee S, Lee JB, Valappil NV, Luo D, Menon VM (2011) Investigating the distance limit of a metal nanoparticle based spectroscopic ruler. Biomed Opt Express 2:1727–1733. https://doi.org/10.1364/BOE.2.001727

Chen Y, Munechika K, Ginger DS (2007) Dependence of fluorescence intensity on the spectral overlap between fluorophores and plasmon resonant single silver nanoparticles. Nano Lett 7:690–696

Cheng C, Sie E, Liu B, Huan C, Sum T, Sun H et al (2010) Surface plasmon enhanced band edge luminescence of ZnO nanorods by capping Au nanoparticles. Appl Phys Lett 96:071107. https://doi.org/10.1063/1.3323091

Deng W, Xie F, Baltar HT, Goldys EM (2013) Metal-enhanced fluorescence in the life sciences: here, now and beyond. Phys Chem Chem Phys 15:15695–15708. https://doi.org/10.1039/C3CP50206F

Dragan AI, Bishop ES, Casas-Finet JR, Strouse RJ, McGivney J, Schenerman MA et al (2012) Distance dependence of metal-enhanced fluorescence. Plasmonics 7:739–744. https://doi.org/10.1007/s11468-012-9366-0

Dulkeith E, Ringler M, Klar T, Feldmann J, Munoz Javier A, Parak W (2005) Gold nanoparticles quench fluorescence by phase induced radiative rate suppression. Nano Lett 5:585–589. https://doi.org/10.1021/nl0480969

Emam A, Mohamed M, Girgis E, Rao KV (2015) Hybrid magnetic–plasmonic nanocomposite: embedding cobalt clusters in gold nanorods. RSC Adv 5:34696–34703. https://doi.org/10.1039/C5RA01918D

Emam AN, Mansour AS, Girgis E, Mohamed MB (2017a) Hybrid nanostructures: synthesis and physicochemical characterizations of plasmonic nanocomposites. Applying Nanotechnology for Environmental Sustainability: IGI Global:231–275

Emam A, Loutfy SA, Mostafa AA, Awad H, Mohamed MB (2017b) Cyto-toxicity, biocompatibility and cellular response of carbon dots–plasmonic based nano-hybrids for bioimaging. RSC Adv 7:23502–23514. https://doi.org/10.1039/C7RA01423F

Emam A, Mostafa A, Mohamed M, Gadallah A-S, El-Kemary M (2018) Enhancement of the Collective Optical Properties of Plasmonic Hybrid Carbon Dots via Localized Surface Plasmon. J Lumin 200:287–297. https://doi.org/10.1016/j.jlumin.2018.03.045

Eustis S, El-Sayed MA (2006) Why gold nanoparticles are more precious than pretty gold: noble metal surface plasmon resonance and its enhancement of the radiative and nonradiative properties of nanocrystals of different shapes. Chem Soc Rev 35:209–217. https://doi.org/10.1039/B514191E

Fales AM, Yuan H, Vo-Dinh T (2011) Silica-coated gold nanostars for combined surface-enhanced Raman scattering (SERS) detection and singlet-oxygen generation: a potential nanoplatform for theranostics. Langmuir 27:12186–12190. https://doi.org/10.1021/la202602q

Feng AL, You ML, Tian L, Singamaneni S, Liu M, Duan Z et al (2015) Distance-dependent plasmon-enhanced fluorescence of upconversion nanoparticles using polyelectrolyte multilayers as tunable spacers. Sci Rep 5:7779. https://doi.org/10.1038/srep07779

Ferrando R, Jellinek J, Johnston RL (2008) Nanoalloys: from theory to applications of alloy clusters and nanoparticles. Chem Rev 108:845–910. https://doi.org/10.1021/cr040090g

Gadallah A, Mohamed MB, Azzouz I (2013) Effect of silver NPs plasmon on optical properties of fluorescein dye. Opt Laser Technol 52:109–112. https://doi.org/10.1016/j.optlastec.2013.04.007

Gandra N, Portz C, Tian L, Tang R, Xu B, Achilefu S et al (2014) Probing Distance-Dependent Plasmon-Enhanced Near-Infrared Fluorescence Using Polyelectrolyte Multilayers as Dielectric Spacers. Angew Chem 126:885–889. https://doi.org/10.1002/ange.201308516

Geddes CD (2010) Metal-enhanced fluorescence. Wiley, Hoboken

Geddes CD (2013) Metal-enhanced fluorescence. Phys Chem Chem Phys 15:19537. https://doi.org/10.1039/C3CP90129G

Geddes CD, Lakowicz JR (2002) Metal-enhanced fluorescence. J Fluoresc 12:121–129. https://doi.org/10.1023/A:1016875709579

Geddes CD, Asian K, Gryczynski I, Malicka J, Lakowicz JR (2005) Radiative decay engineering (RDE). Radiative decay engineering. Springer, Dordrecht, pp 405–448. https://doi.org/10.1016/j.ab.2004.11.026

Ghosh Chaudhuri R, Paria S (2011) Core/shell nanoparticles: classes, properties, synthesis mechanisms, characterization, and applications. Chem Rev 112:2373–2433. https://doi.org/10.1021/cr100449n

Giba A, Gadallah A-S, Mohamed M, Azzouz I (2015) Spectroscopic laser parameters of Ag/CdTe nanostructure. J Lumin 167:408–412. https://doi.org/10.1016/j.jlumin.2015.07.012

Girgis E, Khalil W, Emam A, Mohamed M, Rao KV (2012) Nanotoxicity of gold and gold–cobalt nanoalloy. Chem Res Toxicol 25:1086–1098. https://doi.org/10.1021/tx300053h

Haes AJ, Van Duyne RP (2002) A nanoscale optical biosensor: sensitivity and selectivity of an approach based on the localized surface plasmon resonance spectroscopy of triangular silver nanoparticles. J Am Chem Soc 124:10596–10604. https://doi.org/10.1021/ja020393x

Haes AJ, Haynes CL, McFarland AD, Schatz GC, Van Duyne RP, Zou S (2005) Plasmonic materials for surface-enhanced sensing and spectroscopy. MRS Bull 30:368–375. https://doi.org/10.1557/mrs2005.100

Henson J, DiMaria J, Paiella R (2009) Influence of nanoparticle height on plasmonic resonance wavelength and electromagnetic field enhancement in two-dimensional arrays. J Appl Phys 106:093111. https://doi.org/10.1063/1.3255979

Homan KA, Chen J, Schiano A, Mohamed M, Willets KA, Murugesan S et al (2011) Silver–polymer composite stars: synthesis and applications. Adv Funct Mater 21:1673–1680. https://doi.org/10.1002/adfm.201001556

Hrelescu C, Sau TK, Rogach AL, Jäckel F, Laurent G, Douillard L et al (2011) Selective excitation of individual plasmonic hotspots at the tips of single gold nanostars. Nano Lett 11:402–407. https://doi.org/10.1021/nl103007m

Hsieh Y-P, Liang C-T, Chen Y-F, Lai C-W, Chou P-T (2007) Mechanism of giant enhancement of light emission from Au/CdSe nanocomposites. Nanotechnology 18:415707. https://doi.org/10.1088/0957-4484/18/41/415707

Hutter E, Fendler JH (2004) Exploitation of localized surface plasmon resonance. Adv Mater 16:1685–1706. https://doi.org/10.1002/adma.200400271

Hwang E, Smolyaninov I, Davis CC (2009) Surface plasmon polariton enhanced fluorescence from quantum dots on nanostructured metal surfaces. International Quantum Electronics Conference: Optical Society of America. pp JThA5. https://doi.org/10.1109/ISDRS.2009.5378009

Jain PK, Huang X, El-Sayed IH, El-Sayed MA (2007) Review of some interesting surface plasmon resonance-enhanced properties of noble metal nanoparticles and their applications to biosystems. Plasmonics 2:107–118. https://doi.org/10.1007/s11468-007-9031-1

Jain PK, Huang X, El-Sayed IH, El-Sayed MA (2008) Noble metals on the nanoscale: optical and photothermal properties and some applications in imaging, sensing, biology, and medicine. Acc Chem Res 41:1578–1586. https://doi.org/10.1021/ar7002804

Jayabal S, Pandikumar A, Lim HN, Ramaraj R, Sun T, Huang NM (2015) A gold nanorod-based localized surface plasmon resonance platform for the detection of environmentally toxic metal ions. Analyst 140:2540–2555. https://doi.org/10.1039/C4AN02330G

Jeong Y, Kook Y-M, Lee K, Koh W-G (2018) Metal enhanced fluorescence (MEF) for biosensors: General approaches and a review of recent developments. Biosens Bioelectron. https://doi.org/10.1016/j.bios.2018.04.007

Ji X, Xiao C, Lau W-F, Li J, Fu J (2016) Metal enhanced fluorescence improved protein and DNA detection by zigzag Ag nanorod arrays. Biosens Bioelectron 82:240–247. https://doi.org/10.1016/j.bios.2016.04.022

Jin R, Cao Y, Mirkin CA, Kelly K, Schatz GC, Zheng J (2001) Photoinduced conversion of silver nanospheres to nanoprisms. Science 294:1901–1903. https://doi.org/10.1126/science.1066541

Jin R, Cao YC, Hao E, Métraux GS, Schatz GC, Mirkin CA (2003) Controlling anisotropic nanoparticle growth through plasmon excitation. Nature 425:487–490. https://doi.org/10.1038/nature02020

Katz E, Willner I (2004) Integrated nanoparticle–biomolecule hybrid systems: synthesis, properties, and applications. Angew Chem Int Ed 43:6042–6108. https://doi.org/10.1002/anie.200400651

Kelly KL, Coronado E, Zhao LL, Schatz GC (2003) The optical properties of metal nanoparticles: the influence of size, shape, and dielectric environment. J Phys Chem B 107:668–677. https://doi.org/10.1021/jp026731y

Khurgin JB, Sun G, Soref RA (2007) Enhancement of luminescence efficiency using surface plasmon polaritons: figures of merit. JOSA B 24:1968–1980. https://doi.org/10.1364/JOSAB.24.001968

Kreibig U, Vollmer M (1995) Theoretical considerations. Optical properties of metal clusters. Springer, London, pp 13–201

Kumar PS, Pastoriza-Santos I, Rodriguez-Gonzalez B, De Abajo FJG, Liz-Marzan LM (2007) High-yield synthesis and optical response of gold nanostars. Nanotechnology 19:015606. https://doi.org/10.1088/0957-4484/19/01/015606

Lakowicz JR (2005) Radiative decay engineering 5: metal-enhanced fluorescence and plasmon emission. Anal Biochem 337:171–194. https://doi.org/10.1016/j.ab.2004.11.026

Lakowicz JR (2013) Principles of fluorescence spectroscopy. Springer, New York

Lakowicz JR, Geddes CD, Gryczynski I, Malicka J, Gryczynski Z, Aslan K et al (2004) Advances in surface-enhanced fluorescence. J Fluoresc 14:425–441. https://doi.org/10.1023/B:JOFL.0000031824.48401.5c

Lakowicz JR, Ray K, Chowdhury M, Szmacinski H, Fu Y, Zhang J et al (2008) Plasmon-controlled fluorescence: a new paradigm in fluorescence spectroscopy. Analyst 133:1308–1346. https://doi.org/10.1039/B802918K

Lee K-S, El-Sayed MA (2006) Gold and silver nanoparticles in sensing and imaging: sensitivity of plasmon response to size, shape, and metal composition. J Phys Chem B 110:19220–19225. https://doi.org/10.1021/jp062536y

Lee K, Hahn LD, Yuen WW, Vlamakis H, Kolter R, Mooney DJ (2011) Metal-enhanced fluorescence to quantify bacterial adhesion. Adv Mater 23:H101–H1H4. https://doi.org/10.1002/adma.201004096

Li C, Zhu Y, Zhang X, Yang X, Li C (2012) Metal-enhanced fluorescence of carbon dots adsorbed Ag@ SiO 2 core-shell nanoparticles. RSC Adv 2:1765–1768. https://doi.org/10.1039/C2RA01032A

Liaw J-W, Chen H-C, Kuo M-K (2014) Comparison of Au and Ag nanoshells′ metal-enhanced fluorescence. J Quant Spectrosc Radiat Transf 146:321–330. https://doi.org/10.1016/j.jqsrt.2014.02.025

Lien NTH, Duong VTT, Duong V, Do Quang H, Nhung TH (2014) Theranostic gold nanoshells: from synthesis to imaging and photothermal therapy applications. Commun Phys 24:63–70. https://doi.org/10.15625/0868-3166/24/3S2/5061

Link S, El-Sayed MA (2003) Optical properties and ultrafast dynamics of metallic nanocrystals. Ann Rev Phys Chem 54:331–366. https://doi.org/10.1146/annurev.physchem.54.011002.103759

Link S, Wang ZL, El-Sayed M (1999) Alloy formation of gold-silver nanoparticles and the dependence of the plasmon absorption on their composition. J Phys Chem B 103:3529–3533. https://doi.org/10.1021/jp990387w

Liu X, Choi B, Gozubenli N, Jiang P (2013) Periodic arrays of metal nanorings and nanocrescents fabricated by a scalable colloidal templating approach. J Colloid Interface Sci 409:52–58. https://doi.org/10.1016/j.jcis.2013.07.018

Mansour AS, Gadallah A-S, Al-Sherbini A-S, Youssef T, Mohamed M (2017) Photoluminescence and photocatalysis of CdSe tetrapods seeded by Au nanoparticles. J Mol Struct 1149:626–631. https://doi.org/10.1016/j.molstruc.2017.08.033

Mayer KM, Hafner JH (2011) Localized surface plasmon resonance sensors. Chem Rev 111:3828–3857. https://doi.org/10.1021/cr100313v

Mei Z, Tang L (2016) Surface-plasmon-coupled fluorescence enhancement based on ordered gold nanorod array biochip for ultrasensitive DNA analysis. Anal Chem 89:633–639. https://doi.org/10.1021/acs.analchem.6b02797

Mie G (1908) Beiträge zur Optik trüber Medien, speziell kolloidaler Metallösungen. Ann Phys 330:377–445. https://doi.org/10.1002/andp.19083300302

Millstone JE, Park S, Shuford KL, Qin L, Schatz GC, Mirkin CA (2005) Observation of a quadrupole plasmon mode for a colloidal solution of gold nanoprisms. J Am Chem Soc 127:5312–5313. https://doi.org/10.1021/ja043245a

Mishra H, Mali BL, Karolin J, Dragan AI, Geddes CD (2013) Experimental and theoretical study of the distance dependence of metal-enhanced fluorescence, phosphorescence and delayed fluorescence in a single system. Phys Chem Chem Phys 15:19538–19544. https://doi.org/10.1039/C3CP50633A

Morton SM, Silverstein DW, Jensen L (2011) Theoretical studies of plasmonics using electronic structure methods. Chem Rev 111:3962–3994. https://doi.org/10.1021/cr100265f

Nagel JR, Scarpulla MA (2010) Enhanced absorption in optically thin solar cells by scattering from embedded dielectric nanoparticles. Opt Exp 18:A139–AA46. https://doi.org/10.1364/OE.18.00A139

Oldenburg S, Averitt R, Westcott S, Halas N (1998) Nanoengineering of optical resonances. Chem Phys Lett 288:243–247. https://doi.org/10.1016/S0009-2614(98)00277-2

Peng J, Li J, Xu W, Wang L, Su D, Teoh CL et al (2018) Silica Nanoparticle-Enhanced Fluorescent Sensor Array for Heavy Metal Ions Detection in Colloid Solution. Anal Chem 90:1628–1634. https://doi.org/10.1021/acs.analchem.7b02883

Piccione B, Aspetti CO, Cho C-H, Agarwal R (2014) Tailoring light–matter coupling in semiconductor and hybrid-plasmonic nanowires. Rep Prog Phys 77:086401. https://doi.org/10.1088/0034-4885/77/8/086401

Pitarke J, Silkin V, Chulkov E, Echenique P (2006) Theory of surface plasmons and surface-plasmon polaritons. Rep Prog Phys 70:1. https://doi.org/10.1088/0034-4885/70/1/R01

Pons T, Medintz IL, Sapsford KE, Higashiya S, Grimes AF, English DS et al (2007) On the quenching of semiconductor quantum dot photoluminescence by proximal gold nanoparticles. Nano Lett 7:3157–3164. https://doi.org/10.1021/nl071729+

Prodan E, Radloff C, Halas NJ, Nordlander P (2003) A hybridization model for the plasmon response of complex nanostructures. Science 302:419–422. https://doi.org/10.1126/science.1089171

Rady ME-KAMMBMANEA-SA-STYH (2018) Remarkable Enhancement of Optical properties and Photocatalytic efficiency of Au-CdSe Tetrapods upon Loading into Graphene Oxide. (not published – in preparation)

Ragab A, Gadallah A-S, Da Ros T, Mohamed M, Azzouz I (2014a) Ag surface plasmon enhances luminescence of CdTe QDs. Opt Commun 314:86–89. https://doi.org/10.1016/j.optcom.2013.10.013

Ragab A, Gadallah A-S, Mohamed M, Azzouz I (2014b) Photoluminescence and upconversion on Ag/CdTe quantum dots. Opt Laser Technol 63:8–12. https://doi.org/10.1016/j.optlastec.2014.03.006

Ran C, Wang M, Gao W, Yang Z, Shao J, Deng J et al (2014) A general route to enhance the fluorescence of graphene quantum dots by Ag nanoparticles. RSC Adv 4:21772–21776. https://doi.org/10.1039/C4RA03542A

Ray K, Badugu R, Lakowicz JR (2006a) Distance-Dependent Metal-Enhanced Fluorescence from Langmuir− Blodgett Monolayers of Alkyl-NBD Derivatives on Silver Island Films. Langmuir 22:8374–8378. https://doi.org/10.1021/la061058f

Ray K, Badugu R, Lakowicz JR (2006b) Metal-enhanced fluorescence from CdTe nanocrystals: a single-molecule fluorescence study. J Am Chem Soc 128:8998–8999. https://doi.org/10.1021/ja061762i

Rodríguez-Oliveros R, Sánchez-Gil JA (2012) Gold nanostars as thermoplasmonic nanoparticles for optical heating. Opt Express 20:621–626. https://doi.org/10.1364/OE.20.000621

Rosi NL, Mirkin CA (2005) Nanostructures in biodiagnostics. Chem Rev 105:1547–1562. https://doi.org/10.1021/cr030067f

Sherry LJ, Jin R, Mirkin CA, Schatz GC, Van Duyne RP (2006) Localized surface plasmon resonance spectroscopy of single silver triangular nanoprisms. Nano Lett 6:2060–2065. https://doi.org/10.1021/nl061286u

Shevchenko EV, Ringler M, Schwemer A, Talapin DV, Klar TA, Rogach AL et al (2008) Self-assembled binary superlattices of CdSe and Au nanocrystals and their fluorescence properties. J Am Chem Soc 130:3274–3275. https://doi.org/10.1021/ja710619s

Shi W, Zeng H, Sahoo Y, Ohulchanskyy TY, Ding Y, Wang ZL et al (2006) A general approach to binary and ternary hybrid nanocrystals. Nano Lett 6:875–881. https://doi.org/10.1021/nl0600833

Skoog DA, Holler FJ, Crouch SR (2017) Principles of instrumental analysis. Cengage learning, Boca Raton

Stoermer RL, Keating CD (2006) Distance-dependent emission from dye-labeled oligonucleotides on striped Au/Ag nanowires: effect of secondary structure and hybridization efficiency. J Am Chem Soc 128:13243–13254. https://doi.org/10.1021/ja0637200

Sun G, Khurgin JB, Soref R (2009) Practical enhancement of photoluminescence by metal nanoparticles. Appl Phys Lett 94:101103. https://doi.org/10.1063/1.3097025

Tesler AB, Chuntonov L, Karakouz T, Bendikov TA, Haran G, Vaskevich A et al (2011) Tunable localized plasmon transducers prepared by thermal dewetting of percolated evaporated gold films. J Phys Chem C 115:24642–24652. https://doi.org/10.1021/jp209114j

Touahir L, Galopin E, Boukherroub R, Gouget-Laemmel AC, Chazalviel J-N, Ozanam F et al (2010) Localized surface plasmon-enhanced fluorescence spectroscopy for highly-sensitive real-time detection of DNA hybridization. Biosens Bioelectron 25:2579–2585. https://doi.org/10.1016/j.bios.2010.04.026

Willets KA, Van Duyne RP (2007) Localized surface plasmon resonance spectroscopy and sensing. Annu Rev Phys Chem 58:267–297. https://doi.org/10.1146/annurev.physchem.58.032806.104607

Wu LY, Ross BM, Lee LP (2009) Optical properties of the crescent-shaped nanohole antenna. Nano Lett 9:1956–1961. https://doi.org/10.1021/nl9001553

Xie F, Baker MS, Goldys EM (2006) Homogeneous silver-coated nanoparticle substrates for enhanced fluorescence detection. J Phys Chem B 110:23085–23091. https://doi.org/10.1021/jp062170p

Xie F, Baker MS, Goldys EM (2008) Enhanced fluorescence detection on homogeneous gold colloid self-assembled monolayer substrates. Chem Mater 20:1788–1797. https://doi.org/10.1021/cm703121m

Xu Y, Lei G, Booker AC, Linares KA, Fleming DL, Meehan K, et al. (2004) Maximizing dye fluorescence via incorporation of metallic nanoparticles in solution. Lab-on-a-Chip: Platforms, Devices, and Applications: International Society for Optics and Photonics; pp 174–85. https://doi.org/10.1117/12.571309

Xu Z, Hou Y, Sun S (2007) Magnetic core/shell Fe3O4/Au and Fe3O4/Au/Ag nanoparticles with tunable plasmonic properties. J Am Chem Soc 129:8698–8699. https://doi.org/10.1021/ja073057v

Xu D-D, Liu C, Li C-Y, Song C-Y, Kang Y-F, Qi C-B et al (2017) Dual Amplification Fluorescence Assay for Alpha Fetal Protein Utilizing Immunohybridization Chain Reaction and Metal-Enhanced Fluorescence of Carbon Nanodots. ACS Appl Mater Interfaces 9:37606–37614. https://doi.org/10.1021/acsami.7b11659

Yeshchenko OA, Dmitruk IM, Alexeenko AA, Kotko AV, Verdal J, Pinchuk AO (2012) Size and temperature effects on the surface plasmon resonance in silver nanoparticles. Plasmonics 7:685–694. https://doi.org/10.1007/s11468-012-9359-z

Yu P, Yao Y, Wu J, Niu X, Rogach AL, Wang Z (2017) Effects of plasmonic metal core-dielectric shell nanoparticles on the broadband light absorption enhancement in thin film solar cells. Sci Rep 7:7696. https://doi.org/10.1038/s41598-017-08077-9

Yuan H, Khatua S, Zijlstra P, Yorulmaz M, Orrit M (2013) Thousand-fold enhancement of single-molecule fluorescence near a single gold nanorod. Angew Chem Int Ed 52:1217–1221. https://doi.org/10.1002/anie.201208125

Zhang J, Fu Y, Chowdhury MH, Lakowicz JR (2007) Metal-enhanced single-molecule fluorescence on silver particle monomer and dimer: coupling effect between metal particles. Nano Lett 7:2101. https://doi.org/10.1021/nl071084d

Zhou X, Xiao X, Xu J, Cai G, Ren F, Jiang C (2011) Mechanism of the enhancement and quenching of ZnO photoluminescence by ZnO-Ag coupling. EPL (Europhys Lett) 93:57009. https://doi.org/10.1209/0295-5075/93/57009

Zhou Z, Huang H, Chen Y, Liu F, Huang CZ, Li N (2014) A distance-dependent metal-enhanced fluorescence sensing platform based on molecular beacon design. Biosens Bioelectron 52:367–373. https://doi.org/10.1016/j.bios.2013.09.013

Zielińska-Jurek A (2014) Progress, challenge, and perspective of bimetallic TiO 2-based photocatalysts. J Nanomater 2014:3. https://doi.org/10.1155/2014/208920